PHYSICAL REVIEW B **66**, 045105 (2002)

Ab initio study of the Cu 2*p* and 3*s* core-level XPS spectra of copper phthalocyanine

S. Carniato,[1] G. Dufour,[1] Y. Luo,[2] and H. Ågren[2]
[1]*Laboratoire de Chimie Physique, Matière et Rayonnement, Université Pierre et Marie Curie*
11 rue Pierre et Marie Curie, 75231 Paris Cedex 05 France
[2]*Theoretical Chemistry, Royal Institute of Technology, SCFAB, S-10691 Stockholm, Sweden*

(Received 12 February 2002; revised manuscript received 26 April 2002; published 18 July 2002)

The x-ray photoelectron spectra (XPS) of copper tetraazaporphyrin (CuTAP), used as a model of copper phthalocyanine(CuPc) are studied by theoretical simulations. The nature of the main and satellite features observed in the XPS Cu 2p and Cu 3s photoelectron spectra are discussed based on the results of the charge-transfer (CT) model and of *ab initio* calculations in the sudden approximation limit. It is shown that the two descriptions of the core level final states can be derived from the two types of approaches. The final-state wave functions given by the CT model are described in a shakedown scenario. This process produces a "well-screened" final $2p^5 3d^{10}\underline{L}$ configuration (L denotes a ligand hole) on the Cu atom together with the core hole, resulting in the main spectral peak. On the other hand, the process where the outer electron stays on the ligand corresponds to the satellite with a poorly-screened $2p^5 3d^9$ character. The *ab initio* calculations, performed on an isolated copper tetraazaporphyrin molecule at the Hartree-Fock (HF) level, the multiconfiguration self-consistent field level, and the hybrid density-functional-theory levels show that the core hole final states (satellite/main peak) can be attributed to valence-valence transitions. We show that a correct intensity distribution of the different features, including the so-called white line and the satellite structures, can be obtained when the electronic relaxation and correlation and the overlap between the ground-state and final-state Slater determinants are explicitly taken into account. It is found that the nature of the main peak is strongly depending on the Ligand-to-Metal charge transfer, on the exchange interaction and on the core-hole–3d-hole interaction energies.

DOI: 10.1103/PhysRevB.66.045105 PACS number(s): 79.60.−i, 33.60.Fy

I. INTRODUCTION

The discovery of high T_c superconductivity[1] materials has stimulated a number of studies on the electronic properties of copper perovskites in which the copper atom is found with four or six oxygen atoms in a square or octahedral arrangement. The knowledge of the electronic structure, i.e., the covalent/ionic nature of copper bonding sites and the band gap origin in these compounds, can be of great importance for understanding the mechanism behind superconductivity. In this context, x-ray photoelectron spectroscopy (XPS) has proven to be particularly useful, as it has provided information on the electronic structure of copper oxides (CuO, Cu_2O) in which the copper can be either in the Cu(II) state with an open-shell 3d band, or in the Cu(I) state with a situation closer to the Cu metal with a full 3d band.

The Cu 2p spectrum of the copper atom in the Cu(II) state has two features separated by about 20 eV due to spin-orbit splitting. Each doublet consists of one intense "main peak" and a broad satellite structure at some 8–12 eV toward higher binding energies. In many cases, for instance for CuO (Refs. 2 and 3) and dihalide copper compounds,[4] the $2p_{3/2}$ satellite exhibits a broad multiplet structure while the $2p_{1/2}$ band presents a symmetric shape. It has been shown that the satellite shape, intensity, and energy separation from the main peak depend significantly on the local symmetry and the nature of the ligands. Such information can thus be used to determine the electronic structure of the considered compounds. The nature of the satellite has been the subject of a long debate, for which various models[4–17] have been proposed. Among them, the charge-transfer model[18] seems to have become the most adopted one in recent years. The charge-transfer (CT) model constitutes a semiempirical approach proposed by Van der Laan *et al.*[4] about 20 years ago based on a configuration-interaction formalism. With this model, one can extract useful information about the valence electronic (covalent/ionic) configurations of systems with strong correlation in their ground and final core-hole states directly from experimental data. In this scheme, the electronic valence configuration of the copper atom in the ground state is described as a mixture of both ionic $3d^9$ and $3d^{10}\underline{L}$ configurations, where L denotes a ligand hole. In the presence of a localized core hole generated by the photoemission process, there are certain probabilities that the outer electron will no longer stay on the ligand as it becomes energetically favorable to transfer from a ligand orbital to the d shell. This shakedown process produces a "well-screened" final $c3d^{10}\underline{L}$ (c denotes a ligand hole) configuration on the Cu atom together with the core hole, resulting in the main spectral peak. On the other hand, the process where the outer electron stays on the ligand corresponds to the satellite with a poorly screened $c3d^9$ character.

The atomic multiplet splitting of the $2p^5 3d^9$ configuration has been invoked[4] to interpret the different shapes of the $2p_{3/2}$ and $2p_{1/2}$ satellites. To reproduce as much as possible the distortion of the satellite feature in the experimental spectrum, relevant parameters such as the energy splitting of the p ligands states and the crystal-field splitting of the 3d levels are considered. However, this traditional picture is broken down for the copper acetylacetonate compound, where the experimental spectrum[5,19] exhibits two bands, both in the

$2p_{3/2}$ and $2p_{1/2}$ regions. Okada *et al.*[19] showed that the main peak originates from one well-screened final state $|2p^5 3d^{10}\underline{L}\rangle$, while the two satellite peaks originate from another well-screened state and a state where a stronger $3d^9$ character is present. This description would suggest that the satellite band of dihalides, oxides, and copper phthalocyanine compounds should be described not by one (multiplet) structure but by two bands with different degrees of $L \rightarrow M$ charge-transfer character. In spite the useful of the CT model to characterize the nature of the chemical bond in the ground state and in the various final core hole states, this model exhibits a lack of predictability, and *ab inito* calculations are thus needed. A few years ago, the CT model was tested against *ab initio* calculations of an isolated copper tetraazaporphyrin (CuTAP) molecule by Carniato *et al.*[20] at both the Hartree-Fock (HF) and multiconfiguration self-consistent field (MCSCF) levels. CuTAP was used as a model for copper phthalocyanine (CuPc), the XPS spectrum[21] of which also exhibits a satellite with multiplet structure on the high-binding-energy side of the narrow intense main line. *Ab initio* calculations showed that the main line corresponds to a state in which a strong $L \rightarrow M$ charge transfer process screens the core hole at the cation site, thereby giving a $3d^{10}\underline{L}$ configuration. The satellite is assigned to a mixture of configurations resulting from Ligand->HOMO and Metal->HOMO shakeup transitions from the deep molecular orbitals to the highest singly occupied molecular orbital (HOMO). Apparently, the *ab initio* theoretical calculations and the CT model give the same description for the final states. It should be pointed out that there are several deficits in the early SCF and MCSCF calculations.[20] For instance, the treatment of the electronic relaxation was incomplete while in the intensity calculation the overlap of the Slater determinants was assumed to be equal to 1. However, the main peak/satellite intensity ratio and the energy gap are crucial parameters necessary to validate such an *ab initio* approach. In the present study, we have thus carried out HF, CI, MCSCF, and density-functional-theory (DFT) calculations for the ground state and core-hole final states of CuTAP with basis sets of moderate quality. The final states in presence of a localized core hole are calculated at different levels of accuracy with inclusion of electronic relaxation and correlation. Intensities have been determined by explicitly calculating the overlap between Slater determinants built from nonorthogonal molecular orbitals. A correct description of the relative intensity between the main line and the satellite is then obtained. The roles of both the electronic relaxation and correlation are discussed.[22,23]

II. EXPERIMENTAL

The x-ray photoelectron spectroscopy measurements were obtained in a KRATOS DS800 apparatus under a residual gas pressure in the 10^{-8}–10^{-9} range. The x-ray source is a nonmonochromatized Mg $K\alpha_{1,2}$ source ($h\nu = 1253.6$ eV). The hemispherical analyzer is operated in the fixed pass energy mode of 40 eV with an energy resolution set at 1.00 eV, as measured for the Ag $3d_{5/2}$ line [full width at half maximum (FWHM)]. The binding energy scale was calibrated with the copper metal Cu $2p_{3/2}$ (932.50 eV), Ag $3d_{5/2}$ (368.00 eV), and Au $4fd_{7/2}$ core levels. Commercial copper phthalocyanine (CuPc) powder was pressed and deposited on the stainless-steel sample holder with silver colloidal glue. The different experimental data were displayed on a common binding energy scale, the CuPc C $1s$ peak being used as the reference for all measurements to take into account the charge effect correction. The experimental Cu $2p$ XPS spectrum, shown in Fig. 1, exhibits a $2p_{1/2}$–$2p_{3/2}$ spin-orbit doublet, each component being composed of a main peak plus satellites. The experimental spectral widths are found to be slightly different for the main peaks of the Cu $2p_{1/2}$ (1.8 eV) and Cu $2p_{3/2}$ (1.6 eV) bands, which is a result of the atomic $L_2L_3M_{4,5}$ Coster-Kronig transitions. For each spin-orbit component, the main peak measured at the lower binding energy is a signature of a residual Cu(I) state, i.e., reflecting a situation closer to the Cu metal, with a full $3d$ band.

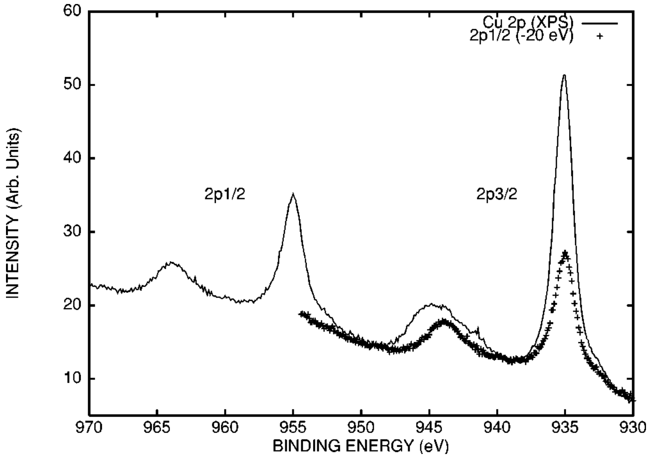

FIG. 1. The experimental CuPc Cu 2p XPS spectrum with the spin-orbit Cu $2p_{3/2}$ and Cu $2p_{1/2}$ main peaks were superimposed.

Similar to what was observed in XPS spectra of copper dihalides, CuO copper oxide or high-T_c superconducting materials, the actual shape of the Cu $2p_{3/2}$ and Cu $2p_{1/2}$ satellite lines in CuPc also present some differences. By superpositioning both the spin-orbit Cu $2p_{3/2}$ and Cu $2p_{1/2}$ main peaks (see Fig. 1), it can be seen that twice of the maximum intensity of the Cu $2p_{1/2}$ satellite line is higher than that of the Cu $2p_{3/2}$. Moreover, a net broadening of the $2p_{3/2}$ component toward higher binding energy appears, while the $2p_{1/2}$ line has a relatively symmetric shape.

Figure 2(a) shows the experimental XPS spectrum of the Cu $3s$ level. The main line at 124.5 eV is followed by a satellite with a maximum intensity centered at about 8.0 eV to the higher-binding energy. The main spectral feature seems to consist of a high intensity peak with large FWMH of 2.6 eV, due to super Coster-Kronig transitions, as fitted by a Voigtian function, and an additional structure at the lower binding energy side corresponding to a Cu(I) state [see Fig. 2(b)]. As clearly shown, attempts to simulate the main feature with two functions of same widths do not allow one to minimize the residuals on the high-binding-energy side of the main peak. Moreover, the experimental spectrum does not show any clear separation between the satellite and the

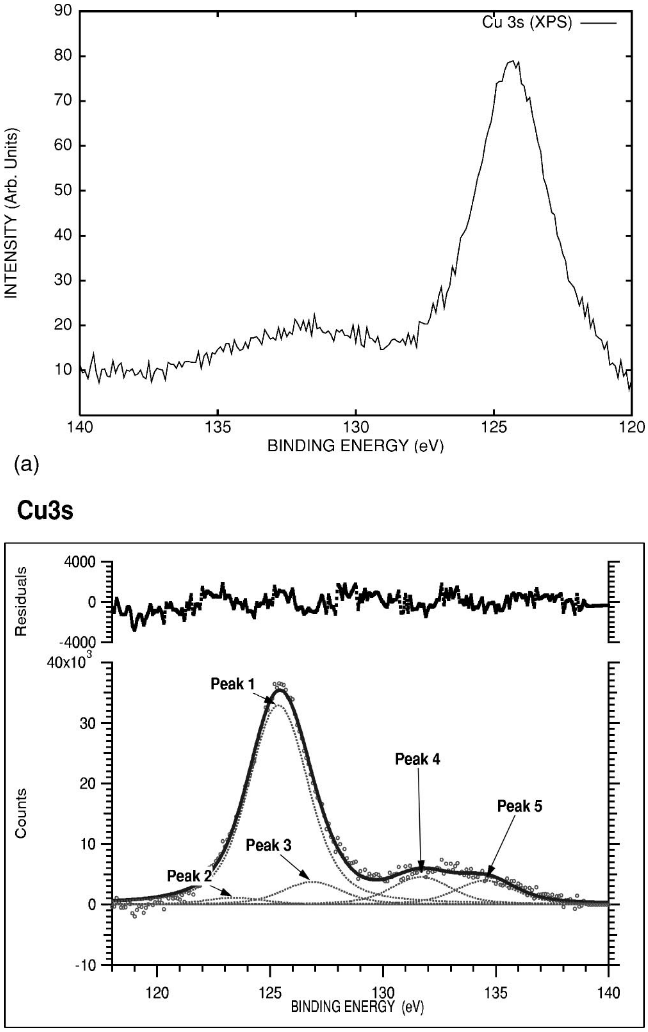

Peak	Area	Energy	Gaussian	Lorentzian
1	1298525	125.3731	2.3530	1.314
2	43351	123.4385	2.3530	1.314
3	146585	126.8731	2.3530	1.314
4	178966	131.6905	2.3530	1.314
5	154360	134.5273	2.3530	1.314

(b)

FIG. 2. The experimental CuPc Cu 3*s* XPS spectrum.

main line, which suggests that some structure on the high-binding-energy side of the main peak exists. In line with the results obtained for cupric complexes such as CuCl$_2$ (Ref. 24) and CuO,[25] the satellite was thus subjectively represented by two well separated components shifted by about 3.0 eV from one another.

III. COMPUTATIONAL DETAILS

Ab initio Hartree-Fock SCF and DFT Kohn-Sham molecular calculations were performed on the copper tetraazaporphyrin (CuTAP), which is a simplified model of Copper Phthalocyanine (CuPc) obtained by replacing the benzene rings of D_{4h} CuPc with hydrogen atoms (see Fig. 3). The free molecule was considered as a reasonable approximation of the multilayer system, where it is expected that intermolecular interactions introduce only a minor perturbation in the local electronic structure around the central atom. The validity of these assumptions has been confirmed by our previous study on the x-ray-absorption spectra of CuPc, in which an excellent agreement between theory and experiment was achieved.[26] The molecular geometry used in the present calculations is based on x-ray data[27] for the β form of CuPc. The crystal structure of CuPc indicates that the molecule is not perfectly D_{4h}. Since the distortion is very small, the choice of a D_{4h} symmetry is still very reasonable and, most importantly, it can reduce the computational time significantly. The D_{4h} averaged geometry reported by Schaffer *et al.*,[28] in which the Cu-N bond lengths are equal to 1.94 Å, has been used. The geometrical structure of the model molecule used in the present study and its atom numbering are displayed in Fig. 3. We define the x and y axes as such that the Cu $3d_{x^2-y^2}$ atomic orbital points toward the neighboring nitrogen atoms.

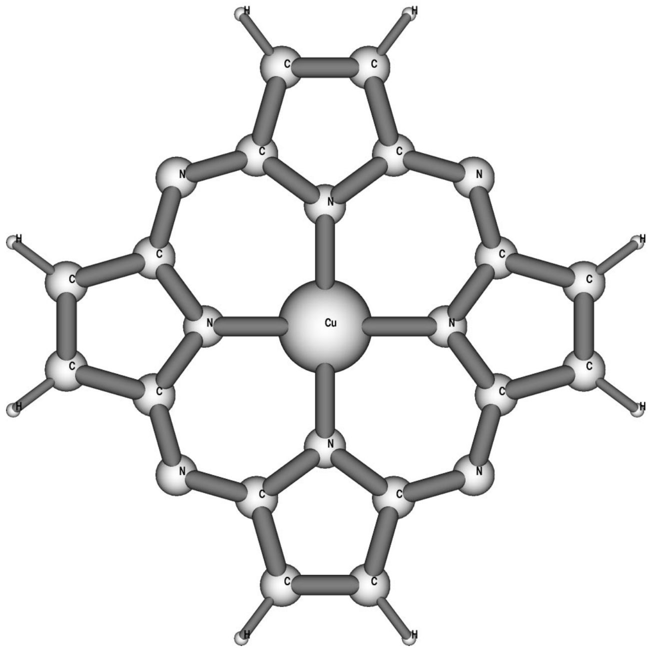

FIG. 3. Idealized D_{4h} structure of square planar copper tetraazaporphyrin (CuTAP).

The XPS Cu 2*p* and Cu 3*s* spectra have been calculated using wave functions of different qualities, SCF plus configuration interaction (CI) and ΔSCF (self-consistent field) (ΔKohn-Sham), taking into account electronic relaxation and correlation explicitly. In the CI calculations, the states are described by a combination of determinants built as follows.

(i) Model 1 ($M1$) Ground-state molecular orbitals.

(ii) Model 2 ($M2$): For the Cu 2*p* hole states, the triplet HF-SCF MO's of the Cu $2p_z$ core ionized state are computed. For each Cu $2p_z$ and Cu $2p_{x,y}$ (singlet and triplet) state a CI calculation is performed with determinants that include excitations between the ligand molecular orbitals and the singly occupied molecular orbital. Due to symmetry reasons, the active space of allowed transitions for the Cu $2p_z$ and Cu 3*s* core inner shells can be restricted to $b_{1g}\rightarrow b_{1g}$.

Additional a_{1g} and b_{2g} MOs were added to the set of b_{1g} Cu $2p_{x,y,z}$ core levels. For Cu $3s$, triplet and singlet lowest HF-SCF energies are separately computed. For each component, a CI calculation including the b_{1g} ligand MO's has been performed.

(iii) Model 3 ($M3$): For Cu $2p$, each triplet HF-SCF or DFT Cu $2p_z$ core-ionized configuration was separately computed. For each HF-SCF singlet[33] Cu $2p_z$ and Cu $2p_{x,y}$ (singlet, triplet) state, a single-determinant CI calculation was performed. We anticipate that such an approach should give a more reliable $3d$ electron population rearrangement as occurring in the core ionized final states.

The active space used for the MCSCF and CI calculations of the ground state of copper tetraazaporphyrin was limited to the singly occupied HOMO ($10b_{1g}$) and the six highest doubly occupied b_{1g} MOs, those are the orbitals directly involved in the possible $L \rightarrow M$ transitions which can occur during the core-level ionization process. Density-functional-theory calculations were performed with the B3LYP exchange-correlation functional and one (BHHLYP) in which the half Hartree-Fock and Becke[29] exchange functionals combined with the correlation functional by Lee, Parr, and Yang[30] was used.

The basis set (Bs1) used in the HF, CI, and MCSCF calculations are 6-31G basis sets for the copper,[31] carbon and nitrogen atoms,[32] and a 3-21G basis set for the hydrogen atoms. At a DFT level of theory, we have also tested larger basis sets.

(i) In the former (Bs2), the 6-31G basis sets for carbon and nitrogen atoms are augmented by a polarization d function (6-31G*). The H ligands are described by a (21/211) polarized basis set.

(ii) In the third basis set (Bs3), Bs2 was used for the ligands, while a TZV basis set was selected for the central copper atom.

All *ab initio* calculations have been carried out using the GAMESS(US) (Ref. 33) package. For the tabulated theoretical results, we have chosen to report the final-state energies with respect to the most stable ionized species, the $^3B_{1u}$ cation. However in solid state compounds, the measured quantities are referenced with respect to the spectrometer Fermi level E_f. To be referenced with respect to the Fermi level, the theoretical core binding energies reported in the figures were thus corrected by the experimental binding energy of the $^3B_{1u}$ state. This choice is justified by the proximity of the measured ultraviolet photoemission spectroscopy[34,35] binding energy corresponding to the molecular first ionization potential to the Fermi level. The analysis of the solid state valence band of the free H_2Pc molecular compounds (not reported in this study) show that the $^3B_{1u}$ states lie at ≈ 3.5 eV from the Fermi level.

A. Spin-orbit coupling

The Cu 2p core-excited spectrum shows a doublet feature due to the strong spin-orbital splitting (~ 20.0 eV). The presence of spin-orbit interaction is often accounted for by superposing two spectra from Cu $2p_{1/2,3/2}$ shifted in energy according to the experimental spin-orbit splitting and assuming a statistical value, here $[(2j+1)]/[(2j'+1)]=\frac{1}{2}$, for the corresponding intensities. We have made the assumption that the Cu $2p_{3/2}$ channel spectrum could be obtained from the nonrelativistic results by subtracting $\frac{1}{3}*20$ eV to the calculated Cu $2p_{x,y}$ ($Y_{1,\pm 1}$) lines, while for the Cu $2p_{1/2}$ channel spectrum $\frac{2}{3}*20$ eV should be added to Cu $2p_z(Y_{1,0})$. The calculated spectra from two separate channels should then be added to give the total spectrum. Because the spin-orbit coupling is rather strong, we expect the Cu $2p_{3/2}$ and Cu $2p_{1/2}$ channels not to overlap.

B. Intensity

The intensities reported for the theoretical Cu $2p$ and Cu $3s$ spectra were calculated based on the "sudden approximation." Such an approach is valid when the kinetic energy of the electron is sufficiently large, so that the hole potential can be considered as being switched on instantly, and the creation of excitations around the hole then reaching a limiting value, the so-called sudden limit. It follows from this assumption that the intensities are determined by the monopolar selection rules.[36] The intensity of a given peak is thus proportional to the square of the overlap between the initial- and final-state wave functions,

$$I \propto |\langle \Psi_{final}^{N-1} | \Psi_{initial}^{N-1} \rangle|^2, \tag{1}$$

where the electron in the core spin orbital has been annihilated from the (frozen) ground-state wave function. At a CI level of theory, both the initial and core hole final states can de developed as a linear combination of several electronic determinants having either $3d^9L^2$ or $3d^{10}L^1$ character. Within model $M1$, ground-state molecular orbitals (GSMO's) are considered. The intensities are thus given by the square of the sum of the product of the coefficients of each configuration (determinants) in the initial and final states. In models $M2$ and $M3$, $\Delta E_{\mathrm{SCF}}(\Delta E_{KS})$ reflects the electronic relaxation (electronic relaxation+relaxation-induced change in correlation) caused by the core hole at the Hartree-Fock (DFT) level, which results from the readjustment of the orbitals in going from the neutral molecule to the ionic molecule. The modification of the potential on the cation site due to the presence of a core hole leads to a large increase of the localization of the d valence shells around the central cation site, and the hybridization between the N $2p$ and Cu $3d$ states is thus strongly affected. Consequently, the molecular orbitals in the initial (ground state) and the final states are no longer orthogonal, and the overlap between the initial state wave function and the different electronic determinants describing the final state wave function should therefore be calculated explicitly. For a molecule like CuTAP one gains a lot by utilizing the high (D_{4h}) symmetry in the intensity calculations.

In model $M2$, the excited states of interest are represented by one or a CI combination of determinants built from a set of core hole ($2p^5$ or $3s^1$) Hartree-Fock SCF molecular orbitals ($C_{ore}H_{ole}$-HF). For the Cu $2p_z$ and Cu $3s$ inner shells, the active space of allowed transitions is restricted to the b_{1g}->HOMO(b_{1g}) monoexcitations.

For the XPS Cu $2p$ core level, the computed spectra are finally convoluted with a Gaussian function of full width (FWHM) of 1.6 eV for the main peak and satellite features. A larger FWHM of 2.6 eV was used for the XPS Cu $3s$ spectra, as experimentally observed.

IV. RESULTS AND DISCUSSION

A. The charge-transfer model

We will first apply the charge transfer (CT) model of Van der Laan *et al.*[4] to the CuTAP compound. In the CT model, the initial state is considered as a linear combination of two configurations, $|3d^9\rangle$ and $|3d^{10}\underline{L}\rangle$, where $\underline{L}$ denotes a ligand-to-metal ($L \rightarrow M$) charge-transfer configuration. This charge transfer from a ligand to a metal orbital is possible only if the symmetry of these states are the same. For CuTAP and CuPc with D_{4h} symmetry, the ligand hole is localized in a b_{1g} orbital. The $L \rightarrow M$ charge-transfer energy between two ionic configurations can be defined as

$$\Delta = \langle 3d^{10}\underline{L}|H|3d^{10}\underline{L}\rangle - \langle 3d^9|H|3d^9\rangle. \tag{2}$$

A mixing matrix element T of the two-level Hamiltonian H is given by

$$T = \langle 3d^9|H|3d^{10}\underline{L}\rangle. \tag{3}$$

Neglecting the overlap, the eigenvalues are obtained as

$$E\pm = Eo + \frac{\Delta}{2} \pm \frac{(\Delta^2+4T^2)^{1/2}}{2}, \tag{4}$$

where $Eo = \langle 3d^9|H|3d^9\rangle$. For a positive value of T, the corresponding eigenfunctions can be written as

$$\Psi(g) = \cos(\Theta)|3d^9\rangle - \sin(\Theta)|3d^{10}\underline{L}\rangle \tag{5}$$

for the ground state, and

$$\Psi(L \rightarrow M) = \sin(\Theta)|3d^9\rangle + \cos(\Theta)|3d^{10}\underline{L}\rangle \tag{6}$$

for the $L \rightarrow M$ charge-transfer state with

$$\tan(2\Theta) = \frac{2T}{\Delta}, \tag{7}$$

the value of Θ being restricted to $0 \leqslant \Theta \leqslant 90°$.

With the help of a term Q, representing the interaction of the core hole with the valence $3d$ hole, the eigenvalues can similarly be written for the final state with a core hole on the copper atom as

$$E_{m,s} = Eo + \frac{\Delta}{2} \pm \frac{[(\Delta-Q)^2+4T^2]^{1/2}}{2}, \tag{8}$$

with the corresponding eigenfunctions

$$\Psi(m) = \cos(\Theta')|c^{-1}3d^9\rangle - \sin(\Theta')|c^{-1}3d^{10}\underline{L}\rangle, \tag{9}$$

$$\Psi(s) = \sin(\Theta')|c^{-1}3d^9\rangle + \cos(\Theta')|c^{-1}3d^{10}\underline{L}\rangle, \tag{10}$$

with

$$\tan(2\Theta') = \frac{2T}{\Delta - Q}, \tag{11}$$

the value of Θ' being restricted to $0 \leqslant \Theta' \leqslant 90°$.

The energy separation between the main peak and the satellite is thus given by

$$W = E_s - E_m = [(\Delta-Q)^2+4T^2]^{1/2}. \tag{12}$$

In the sudden approximation, the intensity ratio of the satellite and the main peak is given by

$$\frac{I_s}{I_m} = \left[\frac{\sin(\Theta')\cos(\Theta) - \cos(\Theta')\sin(\Theta)}{\cos(\Theta')\cos(\Theta) + \sin(\Theta')\sin(\Theta)}\right]^2 = \tan(\Theta'-\Theta)^2. \tag{13}$$

The degree of hybridization in the initial and final states are determined by the parameters Θ and Θ', respectively, which can be calculated by knowing the parameters Δ, T, and Q. It was shown in a previous study[4] that T and Q do not depend much on the characters of the ligands; they were found to be 2.5 and 9.0 eV, respectively. Furthermore, the energy separation W can be determined directly from the experimental spectrum as shown in Fig. 1. A value of 9.0 eV is determined for W using the $2p_{1/2}$ spectral feature because of its sharper spectral bands. Meanwhile, the intensity ratio $I_{Sat.}/I_{Main}$ can also be estimated; it is found to be around 0.4. Using Eq. (13), one can obtain a value of 32° for $\Theta' - \Theta$.

By knowing T, Q, and W, Δ can be obtained from Eq. (13); 1.5 eV. The small Δ gives the values of 37° and 69° for Θ and Θ', respectively. It can be concluded that if one wants to describe the experimental intensity ratio correctly by means of the CT model, the initial state of CuPc should be assumed to involve strong hybridization of the ionic $3d^9$ and $3d^{10}\underline{L}$ configurations. The $3d$ population is estimated to be of 9.36 electrons which is a signature of a covalent character of the Cu-N chemical bond. A similar situation was reported previously in a study[22] of the Cu-N conductive organic salt.

In the core hole state, the CT model predicts that the creation of a $2p$ core hole raises the $|\underline{c}3d^9\rangle$ level relative to the $|\underline{c}3d^{10}\underline{L}\rangle$ level due to the strong core-hole–$3d$-hole Coulombic repulsion energy Q. The value of 69° for Θ' shows that the lowest-lying final state is mainly of $\underline{c}3d^{10}\underline{L}$ character.

B. Quantum-chemical calculations

We will determine the characters of the initial and final states by using various modern quantum-chemical methods and compare them with those estimated by the CT model described above.

1. Character of the ground state

The SCF, MCSCF, and DFT ground-state (GS) calculations all show that the ground state of CuTAP is a doublet state with B_{1g} symmetry in the D_{4h} point group. The HOMO is singly occupied and mainly localized on the center copper atom with antibonding character between Cu $3d_{x^2\text{-}y^2}$ and N

TABLE I. Low-lying SCF and DFT $^2B_{1g}$ states of CuTAP with basis sets of different qualities (Bs1, Bs2, Bs3) (see the text).

	Bs1 [a, b, c]		Bs2 [a, b, c]		Bs3 [a, b, c]	
HF-SCF	-2684.396(8.99)		-2684.880(8.97)	0.00	-2685.119(9.17)	0.00
HF+CI	-2684.396	0.00				
	-2683.817	15.76				
	-2683.596	21.77				
MCSCF	-2684.399					
ΔSCF	-2684.396	0.00	-2684.880	0.00	-2685.119	0.00
	-2683.969	11.61	-2684.465	11.30	-2684.717	10.94
	-2683.855	14.70	-2684.360	14.15	-2684.617	13.63
DFT						
BHHLYP	-2691.782(9.00)	0.00	-2692.174(9.00)	0.00	-2692.420(9.30)	0.00
	-2691.467	8.57	-2691.868	8.33	-2691.128	7.95
	-2691.382	10.86	-2691.791	10.42	-2692.054	9.96
B3LYP	-2691.838(9.03)	0.00	-2692.188 (9.04)	0.00	2692.444(9.42)	0.00
	-2691.582	6.97	-2691.939	6.78	-2692.206	6.48
	-2691.518	8.71	-2691.881	8.35	-2692.148	8.05

[a] Total energy.

[b] Energy relative to the $^2B_{1g}$ ground state. In parentheses we give the GS $3d$ Mulliken population.

[c] The two lowest ($L\rightarrow M$) b_{1g}->b_{1g} charge-transfer energies are calculated.

$2p$. These results are in good agreement with the CuPc ESR spectra[37–39] of copper phthalocyanine which exhibit a weak superhyperfine interactions between copper and the nearest-neighbor nitrogens, indicating a moderate mixing between the Cu $3d_{x^2\text{-}y^2}$ and N $2p$ orbitals. To examine the mixing between the one-electron SCF and the $L\rightarrow M$ charge transfer configurations, the wave function of the ground state has been developed as a combination of several electronic determinants having either $3d^9L^2$ or a $3d^{10}L^1$ character; each $L\rightarrow M$ charge-transfer configuration is obtained by promoting an electron from a doubly occupied ligand (b_{1g}) molecular orbital to the HOMO (b_{1g}). Only the case of Bs1 was considered in this study. Calculations were performed at the CI and MCSCF levels. The MCSCF calculations on the CuTAP ground state show that the dominant configuration (more than 99%) is given by the SCF restricted Hartree (ROHF) configuration, with the unpaired electron in the Cu$3d_{x^2\text{-}y^2}$ orbital. The same conclusion can also be drawn from the CI calculations.

Finally, we have also tested the basis set/HF/DFT dependencies of the excitation energies. The energies of few of the lowest $^2B_{1g}$ states are reported in Table I, and compared with HF-SCF/CI/MCSCF calculations. At a HF level of theory, the two lowest $L\rightarrow M$ charge transfer states lie more than 10 eV above the ground state with the formal Cu $3d^9L^2$ configuration. This large energy gap is due to the strong Coulombic repulsion energy between both the electrons localized in the HOMO which exhibits a large Cu metallic character. The calculated DFT energy gaps are more consistent with the value $(\Delta^2+4T^2)^{1/2}$ predicted by the CT model (5.2 eV), which is a signature of the role played by the electronic correlation to reduce the Coulombic repulsion energy. For this purpose, we can see that the energy difference between both the lowest excitated $L\rightarrow M$ charge-transfer states depends weakly on the basis set. However, we note that the exchange-correlation functional has a significant effect on the excitation energies.

The copper $3d$ Mulliken populations given by both the HF and DFT calculations with basis sets of different qualities are also reported. Whatever the basis set is, the HF calculated populations are close to a $3d^9$ configuration. Conversely, a population close to the one predicted by the CT model is obtained by using Bs3 combined with B3LYP exchange-correlation functional. Furthermore, the projection of the BHHLYP and B3LYP DFT GS wave functions onto the one-electron HF-SCF one shows that 97% and 92% is given by the HF-SCF (ROHF) configuration, respectively. We will further discussed the influence of this small hybridization on the main/satellite intensity ratio in core-level XPS spectra of CuPc.

2. Spectral Shapes and Intensities of Cu 2p XPS

The first model we used for calculating the spectral shape and intensity is the one neglecting the orbital relaxation, i.e., model 1. This model can be considered as an extension of the CT model, since in the CT model only one dominant $L\rightarrow M$ transition is included, while in model 1 we have included as many as seven possible $L\rightarrow M$ transitions. Finally, we will present results from the more realistic theoretical approaches, models 2 and 3, and show that the orbital relaxation plays a very important role.

Model 1 (GSMO): The results obtained from model 1 and Bs1 at the *ab initio* CI level can be found in Figs. 4(a) and 4(f). The states of interest are represented by a linear com-

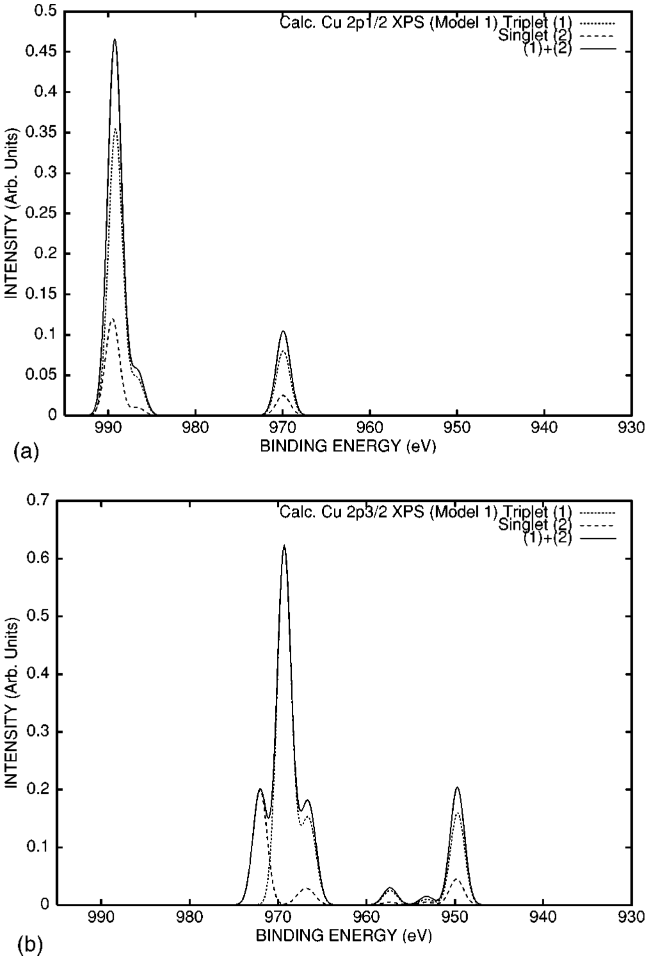

FIG. 4. (a) Calculated Cu $2p_z$ spectrum as a model of the Cu $2p_{1/2}$ spectrum using the configuration interaction (CI) approach and ground-state (GS) molecular orbitals (model $M1$). The origin of the binding energy scale was chosen as described in the text (see Sec. III). (b) Calculated Cu $2p_{x,y}$ spectrum as a model of the Cu $2p_{3/2}$ spectrum using Bs1 (see the text), the configuration interaction (CI) approach, and the ground state (GS) molecular orbitals (model $M1$).

bination of determinants including excitations between the six highest ligand b_{1g} molecular orbitals and the HOMO. For comparison, we have also calculated the energies of the pure unscreened $|\underline{c}3d^9\rangle$ (GS HF-SCF MO's plus a core hole) and the screened $|\underline{c}3d^{10}\underline{L}\rangle$ (i.e., $9b_{1g}$->HOMO charge transfer) final states with Cu $2p_{1/2}$ (Cu $2p_z$) and Cu $2p_{3/2}$ (Cu $2p_{x,y}$) core holes, for both the triplet and singlet configurations. The SCF results show that the one-determinant state of the lowest energy corresponds to a $|\underline{c}3d^{10}\underline{L}\rangle$ screened final state. The CI calculations that take into account the screening caused by electrons from all the inner b_{1g} ligand orbitals also indicate that the lowest state (with low intensity) corresponds to a well screened $L \rightarrow M$ final state resulting from a weak mixing of the reference SCF "unscreened" state and a final state created by an excitation to the HOMO of the outermost doubly occupied molecular orbital. The satellite (the most intense band) is attributed to a poorly screened $|\underline{c}3d^9\rangle$ state. For the Cu $2p_{1/2}$ core hole, the satellite consists essentially of one symmetric peak due to a small singlet-triplet exchange splitting (≈ 0.4 eV). For the Cu $2p_{2/3}$ core levels, the large singlet-triplet exchange splitting (2.85 eV) leads to a multistructure spectral profile in the satellite region.

In general, the calculated results from model 1 are of poor quality, obviously the degree of the hybridization between both the unscreened and well-screened states is close to the one obtained by the CT model. One can find that, with respect to the experimental data, the calculated binding energy value of the lowest energy state differs by more than 10.0 eV and the energy difference between the main peak and the satellite is largely overestimated (≈ 10.0 eV). Moreover, the calculated intensity ratio between the main peak and the satellite is completely wrong. The origin of this large discrepancy is threefold.

(i) The electronic repulsion between both electrons that are strongly localized on the Cu $3d_{x^2\text{-}y^2}$ orbital in the ground state is overestimated at the GSMO+CI level.

(ii) The electronic relaxation is completely neglected for the core hole final states. As a consequence, the sum of the first HF-SCF charge-transfer energy (≈ 15 eV) and the calculated energy difference between the pures $|2p^5 3d^9\rangle$ (satellite) and $|2p^5 3d^{10}\underline{L}\rangle$ (main peak) core-hole final states provides thus an estimate of the Coulombic $2p$-$3d$ interaction energy (more than 30.0 eV) which is largely overestimated with respect to the parametrized CT value.

(iii) Because a relative small CI, the electronic correlation treatment is poor both for the ground state and the core-hole final states, respectively.

It can be concluded that a model without orbital relaxation should not be used to describe the XPS spectra of CuPc.

Models 2 and 3: In Figs. 5(a) and 5(b), we report the results obtained from models M2 and M3 that include different levels of orbital relaxation. The use of the cation MO's of the core-ionized molecule is expected to provide the correct electron rearrangement in the final state. In model 2, the lowest HF-SCF core-hole state obtained by ionization of the neutral CuTAP molecule from the Cu $2p_z$ inner shell is calculated. For each single-determinant core-ionized configuration, including the lowest SCF Cu $2p_z$ state and the b_{1g}-b_{1g} excitations between the ligand MO's and the singly occupied molecular orbital, the value of the corresponding overlap between the GS and the B_{1g} sub-Slater determinants were calculated. Then a CI procedure as previously described is performed to calculate the complete set of Cu $2p_z$ (1/2) and Cu $2p_{x,y}$ (3/2) singlet and triplet states. When the core hole is produced, a large increase of the localization of the $3d$ atomic orbitals on the Cu metal occurs. In contrast to the ground-state picture where the HOMO is strongly localized on the metal (Cu $3d_{x^2\text{-}y^2}$), the creation of a $2p$ core hole is followed by a strong localization of the Cu $3d_{x^2\text{-}y^2}$ character into the inner ligands b_{1g} orbitals, allowing hybridization between the in-plane metal Cu $3d_{x^2\text{-}y^2}$ and the nitrogen N $2p$. Meanwhile, the outermost singly occupied b_{1g} orbital becomes more ligandlike. The appropriate excited core-hole state configurations obtained by promoting an electron from a deeper doubly occupied MO to the singly occupied MO thus correspond to transitions from both ligand centered and

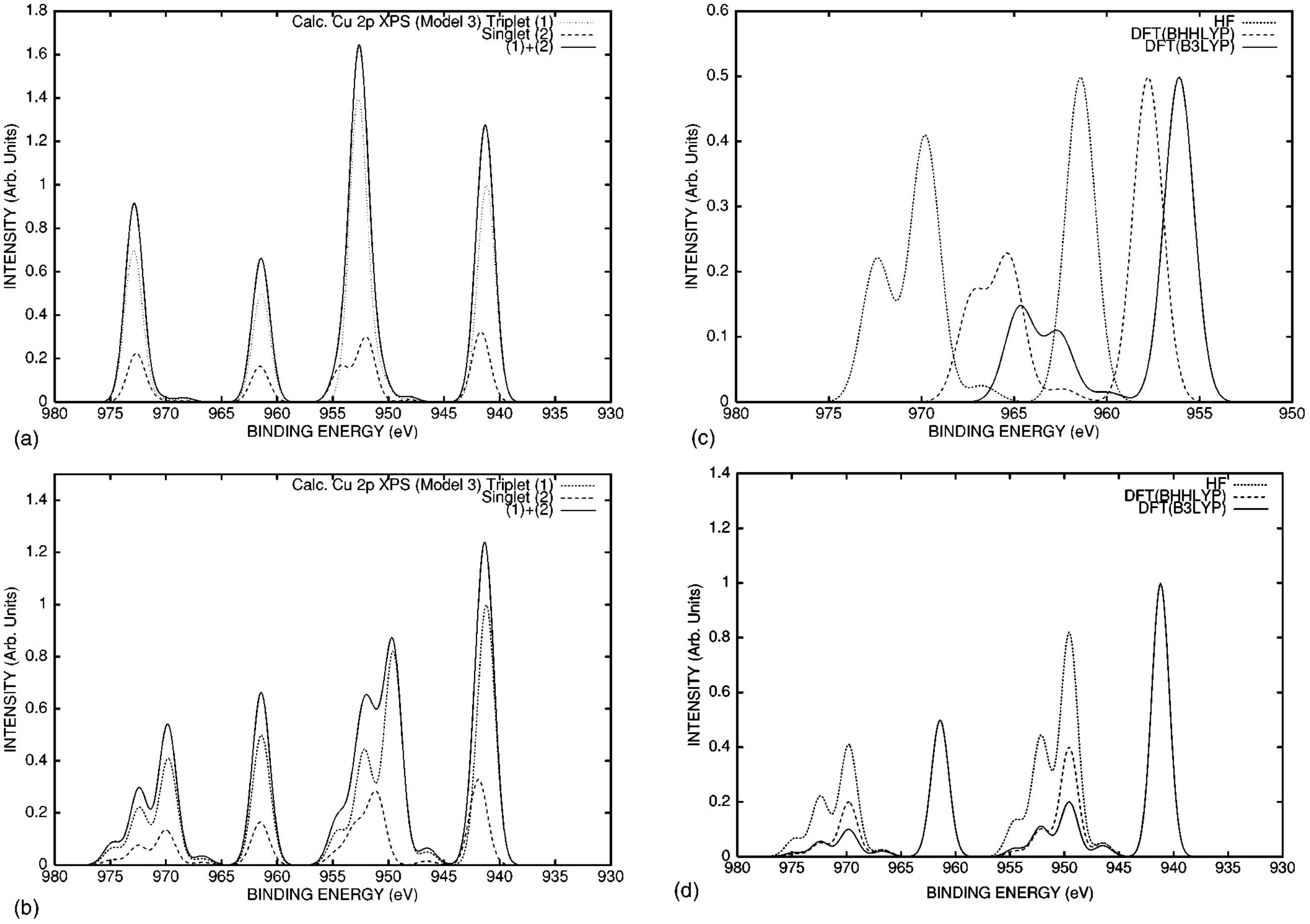

FIG. 5. (a) Calculated Cu $2p_z$ and Cu $2p_{x,y}$ spectra as models of the Cu $2p_{1/2}$ and Cu $2p_{3/2}$ spectra using Bs1 (see the text), a configuration interaction (CI) approach and the triplet Cu $2p_z$ molecular orbitals as reference (model 2). A Gaussian line with a full width at half maximum of 1.6 eV was used for all the bands contributing to the spectra. (b) Calculated Cu $2p_z$ and Cu $2p_{x,y}$ spectra as models of the Cu $2p_{1/2}$ and Cu $2p_{3/2}$ spectra. Within $M3$, each triplet HF-SCF Cu $2p_z$ core-ionized configuration was separately computed. For each singlet Cu $2p_z$ and Cu $2p_{x,y}$ (singlet and triplet) state, a single-determinant CI calculation was thus performed. (c) Theoretical triplet Cu $2p_z$ XPS spectra for the CuPc calculated at a ΔSCF and a ΔKS (Kohn-Sham) DFT (with BHHLYP and B3LYP exchange-correlation functionals) levels of theory. (d) Theoretical triplet Cu $2p_{3/2}(xy) -$ Cu $2p_{1/2}(z)$ XPS spectra for the CuPc: for the final state, the HF core hole final state wave functions were used. Three different wave-functions for the initial state were considered: (A) HF, (B) DFT(BHHLYP), and (C) DFT(B3LYP).

metal-localized molecular orbitals.[20] As displayed in Fig. 5(a), the theory vs experiment intensity ratio is better than that obtained with model 1 (the GSMO). However, each satellite feature presents only one symmetric band, which is quite different from the experimental spectrum shown in Fig. 1. This probably indicates that the electron relaxation has not been fully recovered by model 2, a scenario that is further examined by model 3.

In the following, we will discuss the results obtained from model 3 in detail. It is known that when a core hole is created, the strong $2p$-$3d$ Coulombic interaction leads to a strong $L \rightarrow M$ charge transfer from the outermost ligand orbital centered at N $2p$. The calculations show (see Table II), that there is a net increase of the $3d$ population for the lowest core-hole state in comparison with the ground state, which is clearly in favor of a final $\underline{c}3d^{10}\underline{L}$ configuration for the main peak. In addition, we can note that the absolute theoretical binding energy values and the energy separation between the satellite and the main peak are in better agreement with the experimental data, which is a clear indication of the important role played by the electronic relaxation effect. In order to calculate the intensity ratio I_s/I_m, the overlap (see Table II) between the ground state and the various triplet Cu $2p_z$ SCF final-state Slater determinants has been computed. The calculated spectra reported in Fig. 5(b) (a Gaussian FWHM of 1.6 eV was used for each state contributing to the Cu $2p$ spectrum) show that a good agreement between the theoretical and experimental XPS Cu $2p$ spectra is nicely obtained.

We have found more than one band in the satellite regions of Cu $2p_{3/2,1/2}$. Such observations seem to be consistent with early measurements of Frost *et al.*[5] and Okada *et al.*,[19] in which that the Cu $2p_{1/2}$ XPS spectra of copper cupric complexes show at least two satellite structures. By inspecting the $3d$ Mulliken population on the copper atom, reported in Table II, we have noted that each state is associated with a strong charge-transfer screening, including the main peak

TABLE II. ΔSCF(ΔKS) Cu 2p CuTAP XPS spectrum.

	Cu $2p_{1/2}$		Cu $2p_{3/2}$			
State	E (eV) [a, b]	HF ΔE (eV) [c, d]	HF E (eV) [a]	SCF ΔE (eV) [c, d]	Overlap [(e, f, g), (h, i)]	population [j]
(1,T)	957.92(954.38,952.64)	0.00(1.00)	937.70	0.00(2.00)	0.64(0.65,0.74),(0.64,0.83)	9.80(9.77,9.75)
(2,T)	963.23(958.88,956.64)	5.31(0.05)	942.99	5.29(0.10)	0.14(0.15,0.15),(0.17,0.14)	9.93(9.90,9.86)
(3,T)	966.30(961.79,959.13)	8.38(0.79)	946.08	8.38(1.59)	0.57(0.55,0.49),(0.50,0.38)	9.47(9.58,9.63)
(4,T)	968.90(963.74,961.25)	10.98(0.39)	948.67	10.97(0.78)	0.40(0.49,0.42),(0.63,0.47)	9.69(9.55,9.50)
(5,T)	971.28(966.09,963.37)	13.36(0.13)	951.04	13.34(0.26)	0.18(0.05,0.04),(0.01,0.01)	9.89(9.91,9.88)
(1,S)	958.02	0.10(0.33)	938.40	0.70 (0.66)		
(2,S)	963.23	5.31(0.02)	943.04	5.34 (0.03)		
(3,S)	966.51	8.59(0.26)	947.59	9.89 (0.53)		
(4,S)	969.00	11.08(0.13)	949.44	11.74(0.26)		
(5,S)	971.30	13.38(0.04)	951.19	13.49(0.09)		

[a] HF binding energies with respect to the lowest open-shell cation $^3B_{1u}$ (-2684.167 a.u.).

[b] In parenthesis are given the DFT calculated core level Cu $2p_z$ core-level binding energies. Relative energy with respect to the open-shell cation $^3B_{1u}$ calculated at a DFT level of theory (-2691.512 a.u. for BHHLYP and -2691.564 u.a. for B3LYP).

[c] Relative energy with respect to the lowest HF-SCF binding energy.

[d] Sudden approximation intensity. Intensities are given by the square of the product of sub-Slater determinants (for the initial and final states) of b_{1g} symmetry. The intensity of the corresponding state is indicated in parenthesis.

[e] ⟨HF(FINAL STATE) | HF(GROUND STATE)⟩ overlap.

[f] ⟨DFT(BHHLYP) | HF(GROUND STATE)⟩ overlap.

[g] ⟨DFT(BHHLYP) | DFT(GROUND STATE)⟩ overlap.

[h] ⟨DFT(B3LYP) | HF(GROUND STATE)⟩ overlap.

[i] ⟨DFT(B3LYP) | DFT(GROUND STATE)⟩ overlap.

[j] HF $3d$ Mulliken electronic population. In parenthesis are given BHHLYP and B3LYP $3d$ Mulliken populations, respectively.

state and all satellite states. In particular, a substantial $L \rightarrow M$ charge transfer of $0.5e$ takes place for the $|\underline{c}3d^9\rangle$ final state, which is usually attributed to an unscreened state. The large $L \rightarrow M$ electronic relaxation is thus sufficient to reduce significantly (by ≈ 10 eV) the main/satellite energy difference as well as the singlet-triplet exchange splitting values between the localized core hole and the valence hole observed in a pure $|\underline{c}3d^9\rangle$ as described in the GSMO free relaxation model

(i) For the Cu $2p_{1/2}$ satellite states, the singlet-triplet separation energy is small and close to the value given by the GSMO model. It is due to the weak exchange interaction between the out-of-plane core level Cu $2p_z$ and the in plane Cu $3d_{x^2\text{-}y^2}$ valence level. The two bands are thus attributed to charge-transfer states that refer to various inner doubly occupied molecular orbitals.

(ii) For the Cu $2p_{3/2}$ (x,y) part, it can be seen that the larger singlet-triplet exchange splitting (≈ 2.85 eV) calculated by model 1 is severely reduced by the inclusion of the electronic relaxation; however, a strong relation can still be found between the $3d$ electron population (9.50, 9.71) and the singlet-triplet splitting-exchange value (1.5, 0.77 eV) of both satellite states. The residual exchange splitting is thus responsible for the spectral broadening toward the high binding energy of the $2p_{3/2}$ satellite band. This picture is also in agreement with the theoretical results of Okada *et al.*, which showed that, in contrast to traditional assignments in which the satellite is attributed to a pure unscreened $|2p^5 3d^9\rangle$ state, the satellite bands were found to be formed by a well-screened $|\underline{c}3d^{10}\underline{L}\rangle$ together with a poorly screened state.

Our calculations have clearly shown that the electronic relaxation plays a major role in providing an accurate description for the intensities of both the main peak and the satellite bands. It should also be noted that the calculated HF-SCF ratio between main and satellite bands is still slightly higher than the experimental one. In Fig. 5(c) we have displayed the HF-SCF and the DFT triplet[33] Cu $2pz$ calculated XPS spectra, using exchange-correlation functionals of different qualities (B3LYP, BHHLYP). The calculated spectra were convoluted with a normalized Gaussian function of full width (FWHM) of 1.6 eV. The HF-SCF main/satellite intensity ratio and the computed binding energies are systematically overestimated vs experiments. Conversely, the main/satellite intensity ratio computed with the BHHLYP and the B3LYP exchange-correlation functionals are in quite good agreement with the experimental one measured for the Cu $2p_{1/2}$ and the satellite region exhibits two bands with nearly equal intensity. To analyze the origin of this improvement vs HF-SCF, we have reported the calculated ⟨DFT| HF(GS)⟩ products between the DFT core hole and the HF GS wave functions. These values are reported in Table II and compared with pures ⟨HF| HF(GS)⟩ and ⟨DFT| DFT(GS)⟩ products. In a general case, we can see that the ⟨DFT| HF(GS)⟩ results are close to the ⟨HF| HF(GS)⟩ results, except for the third satellite states with large $3d^9$ character, showing that the small degree of hybridization in the ground state is essential to reproduce the main/satellite intensity ratio with a good accuracy. In Fig.

5(d), we have compared the Cu $2p_{1/2}$ XPS spectra computed by using three different initial wave-functions [HF, DFT(BHHLYP,B3LYP)] and the final HF wave function for which the whole of the core-hole final states is available. Our results show that we can well reproduce the Cu $2p$ XPS in CuPc when the electronic correlation in the ground state is explicitly taken into account.

On the other hand, the calculations show that the $3d$ population of both the most intense satellite bands are nearly equal and close to $3d^{9.5}$, which is clearly in favor of a heavy mixture of final $c3d^{10}\underline{L}$ and $c3d^{9}\underline{L}$ configurations. This approach is fully consistent with the scenario described by Okada *et al.* for the triplet peak feature of Cu $2p$ XPS spectrum of copper acetylacetonate compounds in a CT approach: the leading peak originates mainly from the $2p^5 3d^{10}\underline{L}$ state obtained by an excitation between the outermost doubly occupied molecular orbital and the singly occupied MO. The two most intense satellite bands are due to a strong hybridization between the $|2p^5 3d^9\rangle$ state and the other well-screened $|2p^5 3d^{10}\underline{L}\rangle$ states corresponding to L->M charge transfer excitation between the low-lying doubly occupied molecular orbitals and the singly occupied MO. As an interpretation, the creation of a $2p$ core hole is followed by a strong shifting of the Cu $3d_{x^2\text{-}y^2}$ character in energy to the inner ligand's b_{1g} orbitals, allowing a strong hybridization between the metal Cu $3d_{x^2\text{-}y^2}$ and the nitrogen N $2p$. As a result, the $2p$ XPS satellite splits almost essentially into two bands close in energy. *Ab initio* calculations thus characterize the shape of the Cu 2p XPS satellite peaks by the presence of many bands, close in energy, with different degrees of L->M charge transfer.

3. Cu 3s XPS spectrum

As for Cu 2p, we have performed CI calculations for the Cu $3s$ core XPS spectrum with different levels of treatment of electronic relaxation ($M1$, $M2$, and $M3$). Both triplet and singlet configurations have been computed separately. Within $M1$ and $M2$, the CI includes the SCF state and the determinants corresponding to excitations from the deep, doubly occupied, b_{1g} MO's to the HOMO.

Model 1 (GSMO): Figure 6(a) shows the XPS spectrum from the Cu $3s$ levels calculated with $M1$ and Bs1. The lowest binding energy line at ≈ 131.5 eV is followed by a satellite band split into two components at about 10.0 and 15 eV, respectively. The main peak exhibits two bands [see Fig. 6(a)] with an energy separation of ≈ 0.5 eV between the singlet and the triplet (the most intense band) states. The lowest triplet final state is a heavy mixture of the $|3s^1 3d^9\rangle$ and $|3s^1 3d^{10}\underline{L}\rangle$ pure states since their HF-SCF energy difference is fairly small (2.77 eV). For the triplet state, the $|3s^1 3d^{10}\underline{L}\rangle$ pure state is much lower in energy than the $|3s^1 3d^9\rangle$ state by approximately 7.7 eV, resulting in a small configuration mixing. The lowest binding energy side of the satellite is represented by the triplet states while the high-binding-energy side is characterized by a singlet configuration.

It is worth noting that the GSMO picture is similar to the attributions given by the CT model,[4,24] i.e., the absence of splitting for the main peak is due to the small $L \rightarrow M$ charge-transfer contribution to the final states. In this case the interaction would act between a ligand hole and a metal core hole. The large splitting in the satellite region has been related (see Refs. 4 and 24) to the magnitude of the singlet-triplet exchange interaction between the unpaired $3s$ and $3d$ electrons. As seen in Fig. 6(a), the computed main peak/satellite intensity ratio obtained with $M1$ is poor, similar to what was reported for the Cu $2p$ core level. However, we can see that the computed main/satellite triplet intensities ratio are very different than those provided for the singlet configurations. This clearly reflects a different degree of the ligand-to-metal charge-transfer screening between these two components.

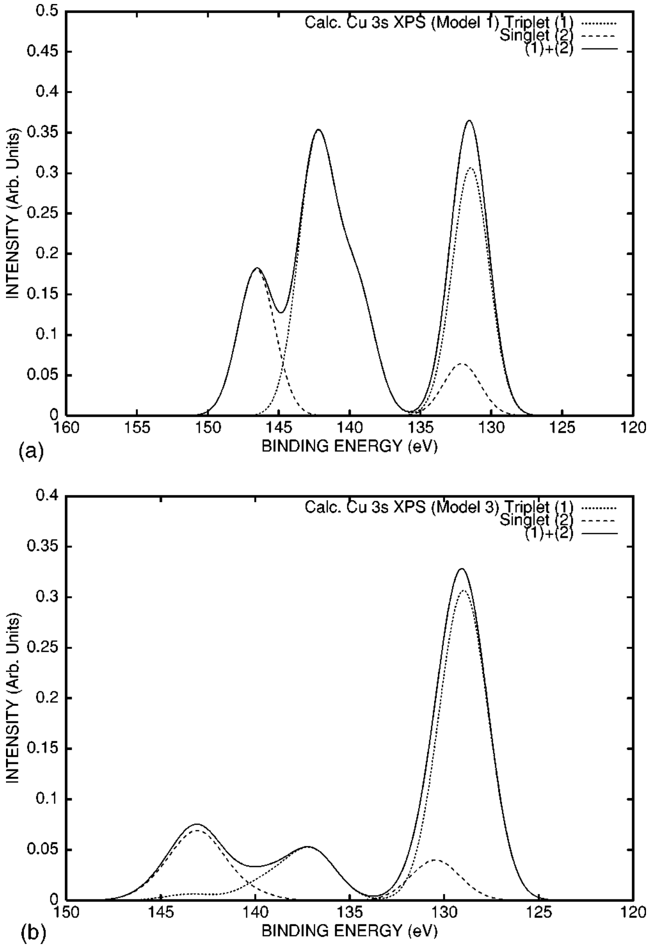

FIG. 6. (a) Theoretical Cu $3s$ XPS spectrum computed with $M1$. A Gaussian with a full width at half maximum of 2.6 eV was used for Cu $3s$ main peaks and satellite states. (b) Theoretical Cu $3s$ XPS spectrum computed with $M2$. A Gaussian with a full width at half maximum of 2.6 eV was used for Cu $3s$ main peaks and satellite states.

Models 2 and 3: We will first discuss some essential $L \rightarrow M$ charge-transfer character of the singlet and triplet states. For the lowest singlet state, the corresponding HF-SCF $3d$ Mulliken population is found to be 9.87 electrons, close to the value for the Cu $2p$ level. This indicates that a strong $L \rightarrow M$ charge transfer is present in a $3s$ core hole state corresponding to the main peak of the spectrum. For the triplet state, the HF-SCF $3d$ population is significantly

TABLE III. ΔSCF Cu 3s CuTAP XPS spectrum.

State	E (eV) [a]	ΔE (eV) [b]	Overlap	Intensity [c]	$3d$ population
(1,T)	125.47	0.00	0.89	1.00	9.44
(2,T)	131.92	6.45	0.14	0.03	9.89
(3,T)	133.97	8.51	0.45	0.25	9.58
(4,T)	137.16	11.69	0.28	0.10	9.77
(5,T)	139.97	14.49	0.07	0.00	9.90
(1,S)	126.96	1.49	-0.55	0.13	9.86
(2,S)	132.00	6.53	0.14	0.00	9.90
(3,S)	136.07	10.60	0.27	0.03	9.86

[a] Relative energy with respect to the lowest open-shell cation $^3B_{1u}$ $(-2684.167\ \text{a.u.})$.

[b] Relative energy with respect to the lowest binding energy.

[c] Sudden approximation intensity.

smaller than that of the singlet, with a value of 9.47 electrons. Thus an $L \rightarrow M$ core-hole charge transfer screening is less effective for the triplet. In spite of the larger charge transfer for the singlet state, the main peak can be characterized by two bands [see Fig. 6(b)] with an energy separation of ≈ 1.5 eV.

The lowest binding energy side of the satellite is represented by a well-screened final triplet $|3s^1 3d^{10}\underline{L}\rangle$ state, while the high binding energy side can be attributed to a singlet configuration where a stronger $3d^9$ character is present. Although an overall agreement between theory and experiment is rather good, $M2$ does not reproduce very well the main peak/satellite energy gap nor the singlet-triplet splitting energy and the intensity ratio between them. A comparative study of the results provided by M2 [Fig. 6(b)] and $M3$ (Table III) for converged triplet and singlet states only, shows that a large amount of the electronic relaxation is missing within $M2$ because only the lowest singlet-triplet core hole relaxed HF-SCF states were explicitly computed with the $M2$ model.

V. SUMMARY

We have studied the x-ray photoelectron spectra (XPS) of copper tetraazaporphyrin (CuTAP) which we used as a model of copper phthalocyanine (CuPc). Results obtained from the semiempirical charge-transfer (CT) model, and *ab initio* theoretical simulations have been discussed. We have shown that, by explicitly including the electron relaxation and the electronic correlation as well as the overlap between the ground- and final-state Slater determinants in the *ab initio* calculations, the main peak/satellite intensity ratio in Cu $2p$ and Cu $3s$ core-level XPS spectra are found to be in quite good agreement with experiment. In particular, the calculations performed at a DFT level of theory have shown that the electronic correlation treatment is essential to reproduce the main/satellite intensity ratio with a good accuracy.

We have found that each of the states (the main line and the satellite features) contributing to the core-level XPS spectra can be characterized by a different degree of ligand-to-metal charge-transfer screening. It is shown that the degree of the $L\text{->}M$ charge transfer characterizing the main peak is strongly depending on the relative energy difference between the ligand-to-metal charge transfer and exchange interaction vs the core-hole–$3d$-hole interaction energy. For the Cu $2p$ XPS, the $2p^5 3d^9$ configuration is raised by the strong core-hole–$3d$-hole repulsion. The main peak thus originates from a well-screened final state $|2p^5 3d^{10}\underline{L}\rangle$, while the satellite peak stems from another well-screened state and a poorly screened state $|2p^5 3d^9\rangle$. In the Cu $3s$ XPS, the final triplet state corresponding to the main peak is characterized by a poor ligand-to-metal charge transfer. The reason for such a small screening can be found in the small core-hole–$3d$-hole repulsion in the $|3s^1 3d^9\rangle$ final configuration with respect to that in the $|2p^5 3d^9\rangle$. Because of a large singlet-triplet exchange interaction the well-screened singlet $3s^1 3d^{10}\underline{L}$ configuration is lower than the $3s^1 3d^9$ in energy. Thus the main peak consists of a poorly screened triplet state and a well-screened charge-transfer singlet state, while the satellite is a combination of a well-screened triplet final state of low binding energy and a poorly screened singlet state at higher binding energy. Our calculations indicate that molecular orbitals optimized in the presence of a core hole in the copper atom provide a reasonable approximation for the electron population relaxation. Our predictive approach can be considered as a reliable alternative to the CT model for describing the chemical bond in the neutral and core hole final states in copper compounds, especially when the satellite states are close in energy.

---

[1] J. Berdnoz and K. A. Müller, Z. Phys. B: Condens. Matter **64**, 18 (1986).

[2] R. F. Roberts, J. Electron Spectrosc. Relat. Phenom. **4**, 273 (1974).

[3] J. Ghijsen, L. H. Tjeng, J. van Elp, J. Eskes, J. Westerink, G. A. Sawatzky, and M.T. Czyzyk, Phys. Rev. B **38**, 11322 (1988).

[4] G. Van der Laan, C. Westra, C. Haas, and G. A. Sawatzky, Phys. Rev. B **23**, 4369 (1981).

[5] D. C. Frost, C. A. McDowell, and R. L. Tapping, J. Electron Spectrosc. Relat. Phenom. **6**, 347 (1975).

[6] A. Rosencwaig, G. K. Wertheim, and H. J. Guggenheim, Phys. Rev. Lett. **27**, 479 (1971).

[7] L. Yin, I. Adler, T. Tsang, M. H. Chen, D. A. Ringers, and B. Crasemann, Phys. Rev. A **46**, 113 (1973).

[8] L. J. Matienzo, L. Yin, S. O. Grim, and W. E. Swartz, Jr. Inorg. Chem. **12**, 2762 (1973).

[9] L. Yin, I. Adler, T. Tsang, L. J. Matienzo, and S. O. Grim, Phys. Rev. Lett. **24**, 81 (1974).

[10] T. Robert and G. Offergeld, Chem. Phys. Lett. **29**, 606 (1974).

[11] D. C. Frost, A. Ishitani, and C. A. McDowell, Mol. Phys. **24**, 861 (1974).

[12] S. Larsson, J. Electron Spectrosc. Relat. Phenom. **8**, 171 (1976).

[13] S. Larsson, Phys. Scr. **16**, 378 (1976); **21**, 558 (1980).

[14] B. W. Veal, D. Ellis, and D. J. Lam, Phys. Rev. B **32**, 5391 (1985).

[15] H. Chen, J. Callaway, and P. K. Misra, Phys. Rev. B **38**, 195 (1988).

[16] F. Parmiggiani, G. Pacchioni, F. Illas, and P. S. Bagus, J. Electron Spectrosc. Relat. Phenom. **59**, 255 (1992).

[17] P. S. Bagus, F. Parmiggiani, and G. Pacchioni, Chem. Phys. Lett. **207**, 569 (1993).

[18] J. D. Lee, O. Gunnarsson, and L. Hedin, Phys. Rev. B **60**, 8034 (1999).

[19] K. Okada, J. Kawai, and A. Kotani, Phys. Rev. B **48**, 10 733 (1993).

[20] S. Carniato, G. Dufour, F. Rochet, H. Roulet, P. Chaquin, and C. Giessner-Prettre, J. Electron Spectrosc. Relat. Phenom. **67**, 189 (1994).

[21] Muralidharan and R. G. Hayes, J. Chem. Phys. **71**, 2970 (1979).

[22] I. H. Inoue, A. Kakizaki, H. Namatame, A. Fujimori, A. Kobayashi, R. Kato, and H. Kobayashi, Phys. Rev. B **45**, 5828 (1992).

[23] Zhi-Xun Shen, J. W. Allen, J. J. Yeh, J.-S. Kang, W. Ellis, W. Spicer, I. Lindau, M. B. Maple, Y. Dalichaouch, M. S. Torikachvili, J. Z. Sun, and T. H. Geballe, Phys. Rev. B **36**, 8414 (1987).

[24] A. A. Gewirth, S. L. Cohen, H. J. Schugar, and E. I. Solomon, Inorg. Chem. **26**, 1133 (1992).

[25] J. C. Cheang-Wong, C. Ortega, J. Siejka, C. Ortiz, M. Sacchi, S. Carniato, G. Dufour, F. Rochet, and H. Roulet, Appl. Sci. Res. **64**, 313 (1993).

[26] S. Carniato, Y. Luo, and H. Ågren, Phys. Rev. B **63**, 085105 (2001).

[27] C. J. Brown, J. Chem. Soc. A **2**, 2488 (1968).

[28] A. M. Schaffer, M. Gouterman, and E. R. Davidson, Theor. Chim. Acta **30**, 9 (1973).

[29] A. D. Becke, Phys. Rev. A **38**, 3098 (1988).

[30] C. Lee, W. Yang, and R. G. Parr, Phys. Rev. B **37**, 785 (1988).

[31] V. Rassolov, J. A. Pople, M. Ratner, and T. L. Windus, J. Chem. Phys. **109**, 1223 (1998).

[32] W. J. Hehre and W. A. Lathan, J. Chem. Phys. **56**, 5255 (1972).

[33] M. W. Schmidt, K. K. Baldridge, J. A. Boatz, S. T. Elbert, M. S. Gordon, J. J. Jensen, S. Koseki, N. Matsunaga, K. A. Nguyen, S. Suand, T. L. Windus, M. Dupuis, and J. A. Montgomery, J. Comput. Chem. **14**, 1347 (1993). The open-shell singlet configurations were not be calculated because the generalized valence bond method (GVB) applied to DFT calculations is not implemented in GAMESS(US).

[34] E. E. Koch and W. D. Grobman, J. Chem. Phys. **67**, 837 (1977).

[35] E. Tegeler, M. Iwan, and E. E. Koch, J. Electron Spectrosc. Relat. Phenom. **22**, 297 (1981).

[36] T. Aberg, Ann. Acad. Sci. Fenn., Ser. A6 **308**, 1 (1969).

[37] W. C. Lin, in *The Porphyrins*, edited by D. Dolphin (Academic Press, New York, 1979), Vol. IV, p. 358.

[38] S. Palacin, A. Ruaudel-Texier, and A. Barraud, J. Phys. Chem. **90**, 6237 (1986).

[39] A. Skorobogaty, R. Lancashire, T. D. Smith, J. R. Pilbrow, and G. R. Sinclair, J. Chem. Soc. Faraday Trans. **79**, 1123 (1983).